

## Fluctuations in superconducting rings with two order parameters

Jorge Berger<sup>1</sup> and Milorad V. Milošević<sup>2</sup>

<sup>1</sup>*Department of Physics and Optical Engineering, Ort-Braude College, P.O. Box 78, 21982 Karmiel, Israel*

<sup>2</sup>*Departement Fysica, Universiteit Antwerpen, Groenenborgerlaan 171, B-2020 Antwerpen, Belgium*

(Received 12 May 2011; revised manuscript received 4 November 2011; published 12 December 2011)

Motivated by two-band superconductivity in, e.g., borides and pnictides, starting from the two-band Ginzburg-Landau energy functional, we discuss how the presence of two order parameters and the coupling between them influence a superconducting ring in the fluctuative regime. Our method is an extension of the von Oppen–Riedel formalism for rings; it is exact, but requires numerical implementation. We also study approximations for which analytic expressions can be obtained, and check their ranges of validity. We provide estimates for the temperature ranges where fluctuations are important, calculate the persistent current in MgB<sub>2</sub> rings as a function of temperature and enclosed flux, and point out its additional dependence on the cross-section area of the wire from which the ring is made. We find temperature regions in which fluctuations enhance the persistent currents and regions where they inhibit the persistent current. The presence of two order parameters that can fluctuate independently always leads to larger averages of the order parameters at  $T_c$ , but yields larger persistent current only for appropriate parameters. In cases of very different material parameters for the two coupled condensates, the persistent current is inhibited.

DOI: [10.1103/PhysRevB.84.214515](https://doi.org/10.1103/PhysRevB.84.214515)

PACS number(s): 74.78.Na, 74.40.-n

### I. INTRODUCTION

Fluctuations are extremely important near phase transitions, and have therefore been the subject of intense research in the past. Particularly in superconductivity, it has been shown that thermally driven electronic fluctuations, i.e., formation and dissociation of Cooper pairs close to the critical temperature  $T_c$ , can affect all relevant properties of a superconductor.<sup>1</sup> Techniques that incorporate thermal fluctuations to the Ginzburg-Landau model are described in a recent review.<sup>2</sup> Fluctuations in mesoscopic loops are particularly interesting because their critical temperature is reduced in an oscillatory fashion as a function of the magnetic field—a phenomenon known as the Little-Parks (LP) effect.<sup>3</sup> More importantly, as LP oscillations are directly related to flux (vorticity) entry in superconductors, one can identify the magnetic fields for which fluctuations are particularly important, as is the case of half integer flux values.<sup>4</sup> The latter experiment<sup>4</sup> detected current in the ring above  $T_c$ , a clear signature of fluctuations, and may be regarded as a paradigm for thin superconducting ring behavior, a case for which the theory for thermal fluctuations is known exactly.<sup>5</sup> The additional influence of quantum fluctuations was addressed in Ref. 6.

Superconductivity is essentially a macroscopic quantum state with long-range phase coherence, therefore described as a single wave function. Superconductors with multiple superconducting gaps, which may therefore be described by multiple order parameters, have recently attracted great attention due to the multigap nature of MgB<sub>2</sub>,<sup>7</sup> OsB<sub>2</sub>,<sup>8</sup> and iron pnictides.<sup>9</sup> In such cases, thermal excitation allows contributions from multiple wave functions and one may expect a dramatically different behavior of the system. With that as motivation, we here explore the interplay of the wave functions and thermal fluctuations in superconducting rings with two order parameters. The rings we will consider need not be made of a two-band superconductor, but may also consist of two thin superimposed superconducting rings,<sup>10</sup> possibly

separated by an isolating layer, such as the active part in readily made experiments with annular Josephson junctions.<sup>11</sup>

We conduct our theoretical analysis in the framework of the Ginzburg-Landau (GL) theory. The multiband GL equations were developed long ago;<sup>12</sup> in the case of two bands the free-energy density has the form

$$f = \sum_{\nu=1,2} \left( \tilde{a}_\nu |\tilde{\Delta}_\nu|^2 + \frac{\tilde{b}_\nu}{2} |\tilde{\Delta}_\nu|^4 + \tilde{K}_\nu |\mathbf{\Pi} \tilde{\Delta}_\nu|^2 \right) - \tilde{\gamma} (\tilde{\Delta}_1 \tilde{\Delta}_2^* + \tilde{\Delta}_2 \tilde{\Delta}_1^*), \quad (1)$$

where  $\tilde{\Delta}_{1,2}$  are the order parameters,  $\tilde{a}_{1,2}$ ,  $\tilde{b}_{1,2}$ ,  $\tilde{K}_{1,2}$ , and  $\tilde{\gamma}$  are material parameters, and  $\mathbf{\Pi} = \nabla + 2\pi i \mathbf{A} / \Phi_0$ , with  $\mathbf{A}$  the vector potential and  $\Phi_0$  the superconducting flux quantum. Zhitomirsky and Dao<sup>13</sup> obtained expressions for the material parameters in a multiband superconductor using Gor'kov's technique. Kogan and Schmalian<sup>14</sup> recently emphasized that consistency imposes conditions on the temperature dependence of these coefficients, which results in the same coherence length for both order parameters in a two-band superconductor. Shanenko *et al.*<sup>15</sup> went on to show the importance of terms of higher order in temperature, and the resulting separation of characteristic lengths for the two bands.<sup>16</sup> We should note, however, that fluctuations move the order parameters astray from equilibrium, so that in general their ratio is not constant.

Moreover, besides clean two-band superconductors, we are also interested in relating our results to additional systems. For example, the functional for two thin superimposed single-band rings, coupled via Josephson tunneling (i.e., Lawrence-Doniach coupling term<sup>17</sup>), will have the shape of Eq. (1), with  $\tilde{a}_\nu^{LD} = \tilde{a}_\nu - \tilde{\gamma}$ . The functional for dirty two-band superconductors will have coefficients with different temperature dependence.<sup>18</sup> In this paper we thus adopt the standard GL approach, where the material parameters in Eq. (1) are arbitrary functions of the temperature and any required restriction will be a particular case. Note, however, that our method is in general applicable to any further modified energy functional,

e.g., for nanothin superconductors (effectively multiband due to quantum confinement of the electron motion, which results in the formation of discrete electronic states and thus splitting of the total band of single-electron states in a series of subbands<sup>19</sup>), dirty two-band superconductors with gradient coupling,<sup>20</sup> or three (or more) -band superconductors.<sup>21</sup>

The paper is organized as follows. In Sec. II we give the details of our theoretical method. In Sec. III we employ different approximations, obtain analytic solutions when possible, and compare to the numerically exact results. Section IV is devoted to properties characteristic of two-order-parameter rings, particularly different degrees of freedom not present in single-band superconductors. We summarize the paper in Sec. V.

## II. METHOD

In this paper we deal with one-dimensional (1D) superconducting rings with two order parameters, extending the results obtained by von Oppen and Riedel<sup>5</sup> (vOR) from single to two order parameters. The vOR formalism is applicable to uniform 1D loops without energy barriers that would sustain metastable states; a method of wider applicability has been presented and explained in detail in Ref. 22.

Instead of the formalism of Ref. 5, we will follow a slightly different approach, which in our view is conceptually simpler, as we will not invoke concepts such as imaginary time or imaginary vector potential. We start by absorbing the coefficients  $\tilde{K}_{1,2}$  into the order parameters and by switching to a gauge invariant formulation, i.e., we define

$$\Delta_v(\theta) = \exp\left(\frac{2\pi i R}{\Phi_0} \int_0^\theta A(\theta') d\theta'\right) \sqrt{\tilde{K}_v} \tilde{\Delta}_v(\theta), \quad (2)$$

where  $R$  is the radius of the ring,  $\theta$  is the angle along the ring, and  $A$  is the tangential component of  $\mathbf{A}$ . Likewise we define

$$a_v = \frac{\tilde{a}_v}{\tilde{K}_v}, \quad b_v = \frac{\tilde{b}_v}{\tilde{K}_v^2}, \quad \gamma = \frac{\tilde{\gamma}}{\sqrt{\tilde{K}_1 \tilde{K}_2}}. \quad (3)$$

With these definitions the free-energy density becomes

$$f = \sum_{v=1,2} \left( a_v |\Delta_v|^2 + \frac{b_v}{2} |\Delta_v|^4 + \frac{1}{R^2} \left| \frac{d\Delta_v}{d\theta} \right|^2 \right) - \gamma (\Delta_1 \Delta_2^* + \Delta_2 \Delta_1^*). \quad (4)$$

With the normalizations we are using,  $a_v^{-1/2}$  is the coherence length for the order parameter  $\Delta_v$  in the absence of coupling to the other order parameter. As in Ref. 5, we consider a uniform 1D ring, which in particular does not alter the applied field (screening is negligible), so that no magnetic energy has to be added to  $f$ .

In order to have a more intuitive picture of the problem, we represent the complex order parameters  $\Delta_v$  by two-dimensional real vectors  $\mathbf{r}_v$ , such that in polar coordinates  $r_v = |\Delta_v|$  and the angular coordinate  $\vartheta_v$  is the phase of  $\Delta_v$ . Integrating  $f$  over the volume of the ring, its free energy becomes

$$F = \frac{2w}{R} \int_{-\pi}^{\pi} d\theta \left( \frac{1}{2} \left| \frac{d\mathbf{r}_1}{d\theta} \right|^2 + \frac{1}{2} \left| \frac{d\mathbf{r}_2}{d\theta} \right|^2 + V \right), \quad (5)$$

where  $w$  is the cross section of the wire from which the ring is made and

$$V = \frac{R^2}{2} \left( a_1 r_1^2 + a_2 r_2^2 + \frac{b_1}{2} r_1^4 + \frac{b_2}{2} r_2^4 - 2\gamma r_1 r_2 \cos(\vartheta_1 - \vartheta_2) \right). \quad (6)$$

As in Ref. 5,  $\mathbf{r}_{1,2}(\theta)$  may be regarded as the trajectories of two fictitious particles during a period of time  $-\pi \leq \theta \leq \pi$ . The first two terms in the integrand of Eq. (5) then represent their kinetic energy and  $V$  their potential energy.

Following Ref. 23, a pair of functions  $\mathbf{r}_v(\theta)$  is interpreted as a microstate of the system and  $F$  as the energy of the system for that microstate. It follows that up to an irrelevant multiplicative constant the partition function is

$$Z = \int \mathcal{D}\mathbf{r}_1 \mathcal{D}\mathbf{r}_2 \exp(-F/k_B T), \quad (7)$$

where  $T$  is the temperature and  $\int \mathcal{D}\mathbf{r}_1 \mathcal{D}\mathbf{r}_2$  denotes integration over all functions  $\mathbf{r}_v(\theta)$  with appropriate periodicity. Since  $\tilde{\Delta}_v$  are single valued,  $r_v(\theta = \pi) = r_v(\theta = -\pi)$  and  $\vartheta_v(\theta = \pi) = \vartheta_v(\theta = -\pi) + 2\pi\varphi$ , where  $\varphi$  is the flux enclosed by the ring divided by  $\Phi_0$ .

Using slight adaptations of Eqs. (2.14), (2.15), (2.16), (2.22), and (2.23) in Ref. 23 (which are reviewed in the appendix),  $Z$  can be brought to the form

$$Z = \sum_n \exp(-2\pi \varepsilon_n / S) \times \int d\mathbf{r}_1 d\mathbf{r}_2 \Psi_n^*[\mathbf{r}_v(\theta = \pi)] \Psi_n[\mathbf{r}_v(\theta = -\pi)]. \quad (8)$$

Here  $\varepsilon_n$  and  $\Psi_n[\mathbf{r}_v]$  are a complete set of eigenvalues and normalized eigenfunctions of the fictitious Hamiltonian

$$H = -\frac{S^2}{2} (\nabla_1^2 + \nabla_2^2) + V, \quad (9)$$

where the Laplacian  $\nabla_v^2$  acts on  $\mathbf{r}_v$  and  $S = k_B T R / 2w$ .  $S$  has dimensions of surface in the plane of the trajectories of  $\mathbf{r}_{1,2}$  and dimensions of force in reality. The integral in Eq. (8) is taken over the entire planes of motion for each particle, but for every argument  $\mathbf{r}_v$  in  $\Psi_n$  we have to take the corresponding argument in  $\Psi_n^*$ .

We note now that the angular momentum operator  $L_z = -i(\partial/\partial\vartheta_1 + \partial/\partial\vartheta_2)$  commutes with  $H$ . We can therefore choose the set of eigenfunctions  $\{\Psi_n\}$  with well defined angular momentum, i.e., they can obey  $L_z \Psi_{n,\ell} = \ell \Psi_{n,\ell}$  and therefore have the form  $\Psi_{n,\ell}(\mathbf{r}_1, \mathbf{r}_2) = \sum_{\ell_1} \psi_{n,\ell,\ell_1}(r_1, r_2, \vartheta_1 - \vartheta_2) \exp\{i[\ell_1 \vartheta_1 + (\ell - \ell_1) \vartheta_2]\}$ , with  $\ell$  and  $\ell_1$  integers. In view of the periodicity conditions of  $\mathbf{r}_v$ , it follows that  $\Psi_{n,\ell}[\mathbf{r}_v(\theta = \pi)] = \exp(2\pi i \ell \varphi) \Psi_{n,\ell}[\mathbf{r}_v(\theta = -\pi)]$ . By substitution of this result into Eq. (8) we obtain

$$Z = \sum_{\ell} \exp(-2\pi i \ell \varphi) Z_{\ell}, \quad (10)$$

with

$$Z_{\ell} = \sum_n \exp(-2\pi \varepsilon_{n,\ell} / S), \quad (11)$$

where summation in Eq. (10) is made over all integers and in Eq. (11) over all the states with total angular momentum  $\ell$ . Since  $H$  is invariant under the transformation  $\{\vartheta_1, \vartheta_2\} \rightarrow \{-\vartheta_1, -\vartheta_2\}$ ,  $\varepsilon_{n,-\ell} = \varepsilon_{n,\ell}$  and we can also write

$$Z = Z_0 + 2 \sum_{\ell=1}^{\infty} \cos(2\pi\ell\varphi) Z_{\ell}. \quad (12)$$

Once the partition function is known, all the equilibrium quantities can be derived from it. The average current around the ring is

$$\langle I \rangle = \frac{k_B T}{\Phi_0} \frac{\partial \ln Z}{\partial \varphi} = -\frac{k_B T}{\Phi_0} \frac{4\pi}{Z} \sum_{\ell=1}^{\infty} \sin(2\pi\ell\varphi) \ell Z_{\ell}. \quad (13)$$

Following similar steps to those that led to Eq. (12), we obtain that the statistical average of any function of the order parameters is

$$\langle p(\Delta_1, \Delta_2) \rangle = \frac{1}{Z} \left[ P_0 + 2 \sum_{\ell=1}^{\infty} \cos(2\pi\ell\varphi) P_{\ell} \right], \quad (14)$$

where  $P_{\ell} = \sum_n \exp(-2\pi\varepsilon_{n,\ell}/S) \langle n\ell | p(\mathbf{r}_1, \mathbf{r}_2) | n\ell \rangle$ . Here we introduced the matrix element  $\langle n\ell | p(\mathbf{r}_1, \mathbf{r}_2) | n\ell \rangle = \int d\mathbf{r}_1 d\mathbf{r}_2 p(\mathbf{r}_1, \mathbf{r}_2) |\Psi_{n,\ell}(\mathbf{r}_v)|^2$ , which may in practice be evaluated in any convenient basis.

### III. EVALUATIONS

All the quantities of interest may be evaluated numerically using Eqs. (10)–(14) of the preceding section. However, if the order parameters are small the problem becomes linearized and simple approximations can be obtained. We therefore postpone the use of Eqs. (10)–(14) to Sec. III C, and first show the analytic results obtained using different approximations.

#### A. High temperature

Let  $T$  be sufficiently higher than  $T_c$ , so that the order parameters are small and the quartic terms in  $V$  can be neglected. For high  $T$  we can also assume  $a_1 + a_2 > \sqrt{(a_1 - a_2)^2 + 4\gamma^2}$  and define the quantities

$$\eta = \frac{a_1 - a_2}{2\sqrt{(a_1 - a_2)^2 + 4\gamma^2}}, \quad (15)$$

$$\xi_{3,4}^2 = \frac{2}{a_1 + a_2 \mp \sqrt{(a_1 - a_2)^2 + 4\gamma^2}}.$$

For  $\gamma = 0$  and  $a_1 > a_2$ ,  $\xi_{3,4} = a_{2,1}^{-1/2}$ ; we therefore regard  $\xi_{3,4}$  as a sort of coherence lengths in the presence of coupling.

We can now define a rotation in the 4D space of both particles through

$$\mathbf{r}_1 = \sqrt{\frac{1}{2} - \eta} \mathbf{r}_3 - \sqrt{\frac{1}{2} + \eta} \mathbf{r}_4, \quad (16)$$

$$\mathbf{r}_2 = \sqrt{\frac{1}{2} + \eta} \mathbf{r}_3 + \sqrt{\frac{1}{2} - \eta} \mathbf{r}_4.$$

With this transformation, the ‘‘potential energy’’ in Eq. (6) becomes

$$V_{\text{quad}} = (R^2/2)[(r_3/\xi_3)^2 + (r_4/\xi_4)^2]. \quad (17)$$

The following features should be noted: (i) in the coordinates  $\{\mathbf{r}_3, \mathbf{r}_4\}$ ,  $\nabla_1^2 + \nabla_2^2$  still has the meaning of the Laplacian in the 4D space; (ii) since on passing from  $\theta = -\pi$  to  $\theta = \pi$  both  $\vartheta_1$  and  $\vartheta_2$  increase by  $2\pi\varphi$ , and since  $\mathbf{r}_{3,4}$  are linear combinations of  $\mathbf{r}_{1,2}$  with fixed coefficients, also their angles  $\vartheta_{3,4}$  increase by  $2\pi\varphi$ ; (iii) the angular momentum operators  $-i\partial/\partial\vartheta_{3,4}$  for each separate particle now both commute with the Hamiltonian; (iv) the total angular momentum equals the sum of the angular momenta of each particle and the total energy equals the sum of their energies. As a consequence of these features, the partition function in Eq. (10) becomes  $Z = Z^{(3)}Z^{(4)}$ , where  $Z^{(v)}$  is the value of  $Z$  obtained when  $\varepsilon_{n,\ell}$  is replaced with the value that corresponds to particle  $v$  only. It follows that equilibrium quantities such as the average current or the average energy will equal the sum of the separate contributions of particles 3 and 4.

The Hamiltonian of the fictitious particles 3 and 4 is just that of two decoupled harmonic oscillators and its eigenvalues are well known:  $\varepsilon_{n,\ell}^{(3,4)} = (SR/\xi_{3,4})(2n + |\ell| + 1)$ . The sum in Eq. (11) becomes a geometric series and we obtain

$$Z_{\ell}^{(3,4)} = \frac{e^{-2\pi|\ell|R/\xi_{3,4}}}{2 \sinh 2\pi R/\xi_{3,4}}. \quad (18)$$

Substitution into Eq. (10) gives

$$Z^{(3,4)} = [2(\cosh 2\pi R/\xi_{3,4} - \cos 2\pi\varphi)]^{-1} \quad (19)$$

and the average current in the ring equals

$$\langle I_{\text{quad}} \rangle = -(2\pi \sin 2\pi\varphi k_B T / \Phi_0) \times [(\cosh 2\pi R/\xi_3 - \cos 2\pi\varphi)^{-1} + (\cosh 2\pi R/\xi_4 - \cos 2\pi\varphi)^{-1}]. \quad (20)$$

From Eq. (20) we can obtain the Little-Parks temperature, i.e., the temperature for the onset of superconductivity in the absence of fluctuations. Without fluctuations the current vanishes above this onset; this is implemented by taking the limit  $k_B T \rightarrow 0$  in the first factor in Eq. (20). At the LP temperature the current becomes nonzero, requiring divergence of the second factor, i.e.,  $iR/\xi_3 = \varphi \bmod 1$ . From here, the LP condition is

$$R^2[\sqrt{(a_1 - a_2)^2 + 4\gamma^2} - (a_1 + a_2)] = 2\varphi^2, \quad (21)$$

where for simplicity of notation we restrict ourselves to the range  $|\varphi| \leq 1/2$ . Near  $T_c$  we can write  $a_v = a_{vc} - \alpha_v \tau$ , with  $\tau = (T_c - T)/T_c$  and  $a_{1c}a_{2c} = \gamma^2$ ; if in addition  $(\varphi/R)^2 \ll \alpha_{1,2}$ , condition (21) is fulfilled for

$$\tau = \tau_{\text{LP}} = \frac{a_{1c} + a_{2c}}{a_{1c}\alpha_2 + a_{2c}\alpha_1} \frac{\varphi^2}{R^2}. \quad (22)$$

#### B. Hartree approximation

One may expect to improve the quadratic approximation by means of a formalism that also becomes exact at  $T = 0$ . For this purpose we make the replacement  $(b_{1,2}/2)r_{1,2}^4 \rightarrow b_{1,2}\langle r_{1,2}^2 \rangle r_{1,2}^2$  in the potential given by Eq. (6). At high temperatures both terms are negligible and at low temperatures, where fluctuations can be neglected, they both lead to the same ‘‘force’’  $-\nabla V$ .<sup>24</sup>

With this approximation the potential becomes again quadratic, so that we can still use the results of the previous section by substituting  $\eta \rightarrow \eta'$  and  $\xi_{3,4} \rightarrow \xi'_{3,4}$ , with

$$\begin{aligned} \eta' &= \frac{a'_1 - a'_2}{2\sqrt{(a'_1 - a'_2)^2 + 4\gamma^2}}, \\ \xi_{3,4}^{\prime 2} &= \frac{2}{a'_1 + a'_2 \mp \sqrt{(a'_1 - a'_2)^2 + 4\gamma^2}}, \\ a'_{1,2} &= a_{1,2} + b_{1,2}\langle r_{1,2}^2 \rangle. \end{aligned} \quad (23)$$

In order to implement this approximation, we have to evaluate  $\langle r_{1,2}^2 \rangle$ .  $\langle r_{3,4}^2 \rangle$  are given by

$$\begin{aligned} \langle r_{3,4}^2 \rangle &= -\frac{S\xi'_{3,4}}{2\pi R^2} \frac{\partial \ln Z^{(3,4)}}{\partial (1/\xi'_{3,4})} \\ &= \frac{S\xi'_{3,4}}{R} \frac{\sinh 2\pi R/\xi'_{3,4}}{\cosh 2\pi R/\xi'_{3,4} - \cos 2\pi\varphi}; \end{aligned} \quad (24)$$

on the other hand, since  $\langle \mathbf{r}_3 \cdot \mathbf{r}_4 \rangle = 0$ ,  $\langle r_{1,2}^2 \rangle = (1/2 \mp \eta')\langle r_3^2 \rangle + (1/2 \pm \eta')\langle r_4^2 \rangle$ , hence  $\langle r_{3,4}^2 \rangle = (1/2 \mp 1/4\eta')\langle r_1^2 \rangle + (1/2 \pm 1/4\eta')\langle r_2^2 \rangle$ . Substituting this into Eq. (24) leads to

$$\begin{aligned} &\left(\frac{1}{2} \mp \frac{1}{4\eta'}\right)\langle r_1^2 \rangle + \left(\frac{1}{2} \pm \frac{1}{4\eta'}\right)\langle r_2^2 \rangle \\ &= \frac{S\xi'_{3,4}}{R} \frac{\sinh 2\pi R/\xi'_{3,4}}{\cosh 2\pi R/\xi'_{3,4} - \cos 2\pi\varphi}. \end{aligned} \quad (25)$$

This is a system of two equations for obtaining  $\langle r_1^2 \rangle$  and  $\langle r_2^2 \rangle$ .

For a general situation, Eqs. (25) have to be solved numerically, but we can find asymptotic expressions for some special situations of interest. Sufficiently above the critical temperature  $T_c$  one usually has  $2\pi R/\xi'_{3,4} \gg 1$ , so that the fractions at the right of Eqs. (25) reduce to 1. Near  $T_c$  and for a range in which  $b_v\langle r_v^2 \rangle \ll \alpha_v|\tau| \ll a_v$  we obtain

$$\begin{aligned} \langle |\Delta_{1,2}|^2(T) \rangle &= \langle r_{1,2}^2 \rangle \\ &\approx \frac{k_B T}{2(a_{1c} + a_{2c})^{3/2} w} \left( a_{1c,2c} + \frac{a_{2c,1c}(a_{1c} + a_{2c})}{\sqrt{(a_{1c}\alpha_2 + a_{2c}\alpha_1)|\tau|}} \right). \end{aligned} \quad (26)$$

It is interesting to note that  $\langle |\Delta_{1,2}|^2(T) \rangle$  decreases very moderately with  $T - T_c$ . If the radius of the ring is sufficiently large, we still have  $2\pi R/\xi'_{3,4} \gg 1$  at  $T = T_c$ ; assuming that  $b_v\langle r_v^2 \rangle \ll a_v$  still holds leads to

$$\begin{aligned} \langle |\Delta_{1,2}|^2(T_c) \rangle &\approx \left( \frac{a_{2c,1c}^2 k_B^2 T_c^2}{4(a_{1c} + a_{2c})\beta_{1,2} w^2} \right)^{1/3} \\ &+ \frac{a_{1c,2c}[3\beta_{1,2} - a_{2c,1c}(b_1 + b_2)]k_B T_c}{6(a_{1c} + a_{2c})^{3/2}\beta_{1,2} w}, \end{aligned} \quad (27)$$

with  $\beta_{1,2} = b_{1,2}a_{2c,1c} + b_{2,1}a_{1c,2c}^3/\gamma^2$ . Comparison of Eqs. (26) and (27) with the values of  $|\Delta_{1,2}|^2$  in the absence of fluctuations enables us to estimate the range of temperatures for which fluctuations are important.

Figure 1 shows the values of  $\langle \Delta_{1,2}^2 \rangle = \langle r_{1,2}^2 \rangle$  near  $T_c$  for MgB<sub>2</sub>, using the material parameters reported in Ref. 25. In the absence of thermal fluctuations,  $\beta_{1,2}\langle \Delta_{1,2}^2 \rangle$  is given by the dashed line for both bands. The inset in the figure shows the

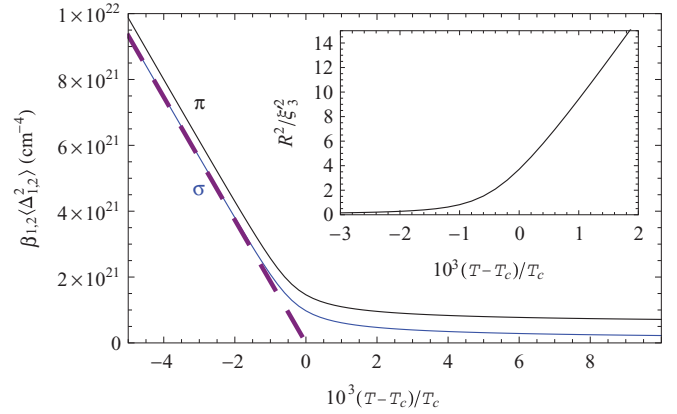


FIG. 1. (Color online) Average Cooper-pair densities  $|\Delta_{v=1,2(=\sigma,\pi)}|^2$  in the ring as functions of temperature, calculated in the Hartree approximation. Each  $|\Delta_v|^2$  has been multiplied by  $\beta_v$  for the purpose of comparison with the values in the absence of thermal fluctuations (dashed line). The sample is a ring of radius  $10^{-4}$  cm and cross section  $10^{-10}$  cm<sup>2</sup> that encloses no magnetic flux. The material parameters are those of MgB<sub>2</sub>, taken from Ref. 25. Inset:  $(R/\xi_3)^2$  for the same ring.

behavior of  $R/\xi_3'$  near  $T_c$ ;  $\xi_4' \ll \xi_3'$  remains practically constant in this range.

Finally, it should be mentioned that, although the Hartree approximation becomes exact both in the limit of high and of low temperature, it has several limitations, and near  $T_c$  the variational Gaussian approximation is expected to be more accurate.<sup>2,26</sup>

### C. Exact evaluation

We proceed now to evaluate numerically the average currents and additional quantities using Eqs. (10)–(14). For this task we require in principle a complete set of eigenvectors and eigenvalues of the Hamiltonian  $H$  in Eq. (9). In practice, the usual procedure invokes some auxiliary Hamiltonian  $H_B$  for which a complete set of eigenvectors and eigenvalues is known.  $H$  is then projected into the subspace of the Hilbert space that has as a basis a set of low energy eigenstates of  $H_B$ . Finally, this projected Hamiltonian is diagonalized numerically and the required eigenvalues are obtained. This procedure is expected to give good approximations for the states of  $H$  that are almost entirely contained in the projection subspace; for this purpose we require a sufficiently large basis and an appropriate choice of  $H_B$ .

We define the basis Hamiltonian

$$H_B(k_1, k_2) = -\frac{S^2}{2}(\nabla_1^2 + \nabla_2^2) + \frac{R^2}{2}(k_1^2 r_1^2 + k_2^2 r_2^2), \quad (28)$$

which has the known set of eigenfunctions

$$\begin{aligned} \psi_{n_1, \ell_1, n_2, \ell_2}(\mathbf{r}_1, \mathbf{r}_2) &= C \prod_{v=1,2} r^{|\ell_v|} e^{-Rk_v r_v^2/2S} \\ &\times {}_1F_1(-n_v, |\ell_v| + 1, Rk_v r_v^2/S) e^{i\ell_v \vartheta_v} \end{aligned} \quad (29)$$

with eigenvalues  $RS[k_1(2n_1 + |\ell_1| + 1) + k_2(2n_2 + |\ell_2| + 1)]$ . Here  $C$  is the normalization constant and  ${}_1F_1$  is Kummer's



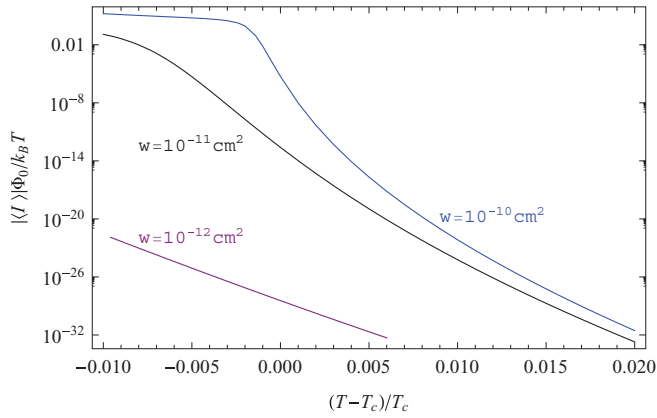


FIG. 2. (Color online) Average current in a two-order-parameter superconducting ring as functions of temperature. For the top curve the parameters are as in Fig. 1, except that the normalized flux is  $\varphi = 0.25$ . For the lower curves the cross section  $w$  of the ring is smaller. The current was evaluated using a truncated basis of the Hilbert space, provided by the functions in Eq. (29) with maximum quantum numbers  $n_{1,\max} = 11$ ,  $|\ell_1|_{\max} = 22$ ,  $n_{2,\max} = 4$ , and  $|\ell_2|_{\max} = 8$ .

hypergeometric function. We can then evaluate any matrix element  $H_{i,j} = \langle \psi_i | H | \psi_j \rangle$ , where the functions  $\psi_{i=1,\dots,N}$  are the functions with lowest eigenvalues within the basis of the Hilbert space provided by Eq. (29). More precisely, when evaluating  $Z_\ell$ , we include in the set  $\{\psi_i\}$  only eigenfunctions that obey  $\ell_1 + \ell_2 = \ell$ . If  $N$  is sufficiently large, then the lowest eigenvalues of the matrix  $(H_{i,j})$  will be a sufficiently accurate approximation for the lowest eigenvalues of the operator  $H$ . In practice, rather than fixing  $N$ , we fix maximum values for  $n_1$ ,  $|\ell_1|$ ,  $n_2$ , and  $|\ell_2|$ .

We are interested in choosing  $k_1$  and  $k_2$  so that an accurate approximation is obtained without  $N$  becoming prohibitively large. From Eq. (29) we see that the scale of  $\langle r_v^2 \rangle$  is given by  $S/Rk_v$ ; we therefore set  $k_v = pS/R\langle r_v^2 \rangle$ , where  $\langle r_v^2 \rangle$  is obtained from the Hartree approximation and  $p$  is still a free parameter. Since for a good approximation the eigenvalues should actually be independent of  $p$ , we mimic this situation by minimizing the lowest eigenvalue of  $(H_{i,j})$  with respect to  $p$ .

Figure 2 shows the currents as functions of the temperature obtained with this method for rings of three different cross sections, with the material parameters of  $\text{MgB}_2$ . For completeness, the figure includes also values of current that are too small to be experimentally observable. The temperature range covered here is much wider than the range presented in Ref. 5, where the temperature scale is given by the Thouless correlation energy (divided by  $k_B$ ) which is of the order of the LP temperature; for a  $\text{MgB}_2$  ring with radius of the order of a micron the LP temperature is of the order of  $10^{-5} T_c$ .

For sufficiently high temperature (the required temperature decreases with cross section  $w$ ), the current becomes independent of the cross section. For the parameters taken here and  $T = 3T_c$ , a ring with  $w = 10^{-10} \text{ cm}^2$  and a ring with  $w = 10^{-8} \text{ cm}^2$  carry the same average current (within 1% difference). At the other extreme, far below  $T_c$ , i.e., where fluctuations are unimportant,  $\langle I \rangle \propto w$ . However, the dependence of  $\langle I \rangle$  on  $w$  near  $T_c$  is not intermediate: we notice in Fig. 2 that decrease of  $w$  by an order of magnitude near

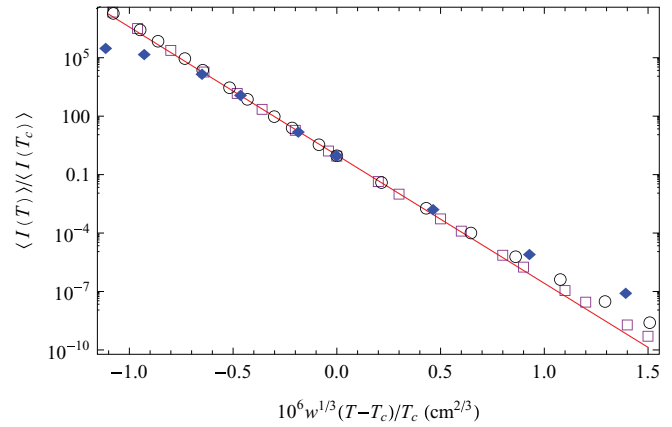


FIG. 3. (Color online) Scaling of the function  $\langle I(T) \rangle$  with the cross section. The parameters are the same as in Fig. 2.  $\blacklozenge$ :  $w = 10^{-10} \text{ cm}^2$ ;  $\circ$ :  $w = 10^{-11} \text{ cm}^2$ ;  $\square$ :  $w = 10^{-12} \text{ cm}^2$ . The straight line is a guide for the eye.

$T_c$  leads to a current decrease of several orders of magnitude, whereas for intermediate behavior the current would decrease by one order of magnitude at most. Figure 3 shows the scaled current against the scaled temperature for the same rings as in Fig. 2, close to  $T_c$ . We notice that, in spite of the moderate influence of temperature on  $\langle |\Delta_{1,2}|^2 \rangle$  predicted by Eq. (26), the current decreases exponentially. We also find that for smaller cross sections the rate of change of  $\langle I \rangle$  is slower. We empirically found that the scaling  $w^{1/3}$  leads to a universal curve.

We attribute didactic interest to understanding the behavior of our methods far below  $T_c$ . There, convergence of the series in Eqs. (12) and (13) becomes slow, and numeric implementation of the exact evaluation becomes inefficient. Below certain temperature,  $\xi_3'^2$  in Eq. (23) becomes negative, and interpretation of the potential in Eq. (17) as that of a harmonic oscillator, and the sum of convergent geometric series that led to Eqs. (20) and (25) is no longer justified. Nevertheless, the expressions in Eqs. (20) and (25) are analytic functions of  $\xi_3'^2$  that remain meaningful and are expected to remain valid beyond the range in which they were proven. Numeric implementation of the Hartree approximation requires special care in order to pick the relevant rather than spurious solutions of Eqs. (25).

In the limit  $T \rightarrow 0$ ,  $R/\xi_3' \rightarrow i\varphi$ , so that the right-hand side in the first of Eqs. (25) does not vanish. Taking the appropriate limits in Eqs. (20) and (25) we obtain that the current in the Hartree approximation is  $I_H(0) = -4\pi w(\Delta_1^2 + \Delta_2^2)\varphi/R\Phi_0$ , exactly as in the absence of fluctuations.

We conclude this section with a review of the accuracy of our evaluations. The accuracy of the “exact” evaluation can be estimated by repeating it with reduced maximum values for  $n_v$  and  $|\ell_v|$ . We found the largest inaccuracy for large  $w$  and small  $T$ . In the results presented in Fig. 2, the maximal inaccuracies are of the order of 10%. Figure 4 compares our approximation methods against the exact evaluation for  $w = 10^{-10} \text{ cm}^2$ . One can see in the figure that all the approximation methods are very inaccurate precisely in the most interesting region, i.e., close to  $T_c$ . The range of temperatures where the approximations are inaccurate is larger for smaller cross sections  $w$ . The Gaussian

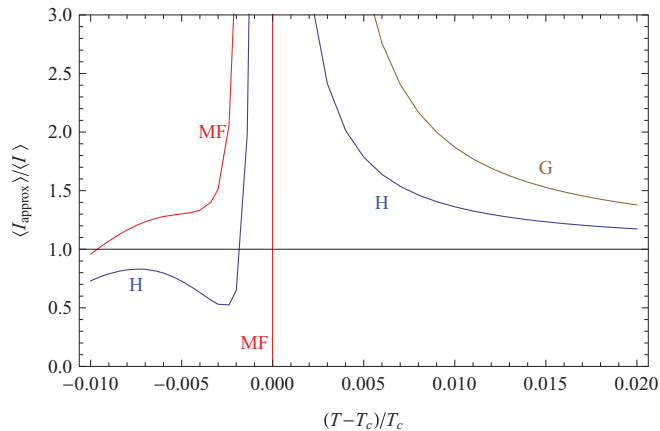


FIG. 4. (Color online) Ratio of the current values obtained with approximated methods to the exact evaluation. Parameters are the same as in Fig. 1, except that here  $\varphi = 0.25$ . G: Gaussian (quadratic) approximation; H: Hartree approximation; MF: mean-field evaluation (i.e., without fluctuations). The descent of the MF curve to 0 at the Little-Parks temperature looks vertical in this scale.

approximation is known to diverge in this region also in the case of a single order parameter.<sup>5,27</sup> Note also that there exists a range of temperatures for which the mean-field current is larger than our exact evaluation, meaning that thermal fluctuations *inhibit the current* in this region.

#### IV. INDEPENDENCE, ASYMMETRY, AND PHASE DIFFERENCE OF THE ORDER PARAMETERS

The most conspicuous qualitative differences of a two order parameter system, as compared to a system with a single order parameter, are *independence* and *asymmetry*. By independence we mean that at a given point and time the two order parameters are not necessarily equal to each other; by asymmetry we mean that the average values of the order parameters are not necessarily the same. A consequence of independence that deserves special attention is that the phases of both order parameters are not necessarily equal. In this section we investigate the influence of these properties.

##### A. Symmetric case

We start by considering independence while assuming equal coefficients for both order parameters. For simplicity, we assume

$$a_v = \gamma - \alpha\tau, \quad b_v = b, \quad (30)$$

with  $\gamma$ ,  $\alpha$ , and  $b$  constants. As an illustration, we may think of a film of a uniform single-parameter material of thickness  $z_0$  with energy density  $-2\alpha\tau|\Delta|^2 + b|\Delta|^4 + 2|\nabla\Delta|^2$ . If we decide to denote by  $\Delta_1$  (respectively  $\Delta_2$ ) the value of  $\Delta$  in the upper (respectively lower) half of the film, substitute the  $z$  derivative by a finite difference and average over  $z_0$ , we obtain the energy density  $-\alpha\tau(|\Delta_1|^2 + |\Delta_2|^2) + b(|\Delta_1|^4 + |\Delta_2|^4)/2 + |\nabla_{xy}\Delta_1|^2 + |\nabla_{xy}\Delta_2|^2 + (8/z_0^2)(|\Delta_1|^2 + |\Delta_2|^2 - \Delta_1\Delta_2^* - \Delta_2\Delta_1^*)$ , with  $\nabla_{xy}$  being the component of the gradient in the plane of the film. One can easily identify that we have recovered the energy density for two order parameters, with coupling

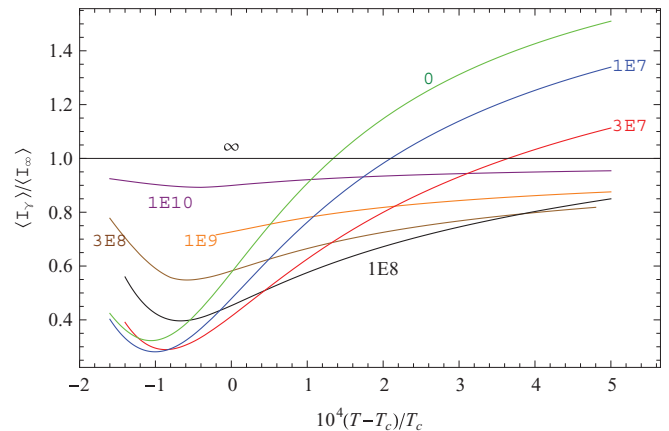


FIG. 5. (Color online) Comparison among currents as functions of the temperature for systems with different coupling  $\gamma$ , but with otherwise identical parameters. The value of  $\gamma$  is marked next to every curve in E notation (e.g., 3E7 denotes  $\gamma = 3 \times 10^7 \text{ cm}^{-2}$ ). The other parameters are  $R = 10^{-4} \text{ cm}$ ,  $w = 10^{-10} \text{ cm}^2$ ,  $\alpha = 10^{12} \text{ cm}^{-2}$ ,  $b = 10^{17} \text{ erg}^{-1} \text{ cm}^{-1}$ ,  $k_B T_c = 10^{-15} \text{ erg}$ ,  $\varphi = 0.25$ .

$\gamma = 8/z_0^2$ . In the limit  $z_0 \rightarrow 0$ ,  $\gamma \rightarrow \infty$ , and  $\Delta_1$  and  $\Delta_2$  are the same; in the opposite extreme,  $\gamma \rightarrow 0$ , and  $\Delta_1$  and  $\Delta_2$  are independent, while in the general case they are correlated. Following this analogy, it is very easy to obtain results for the cases  $\gamma \rightarrow 0$  and  $\gamma \rightarrow \infty$ : the case  $\gamma \rightarrow 0$  is equivalent to that of two single parameter systems in parallel, and the case  $\gamma \rightarrow \infty$  is equivalent to that of a single parameter system with a doubled cross section.

Figure 5 compares calculated average currents  $\langle I(T) \rangle$  as the parameter  $\gamma$  is varied in the range  $0 \leq \gamma < \infty$ , while all the other parameters are common to all curves. For a facilitated comparison, all the functions have been divided by  $\langle I_\infty(T) \rangle$ , the current obtained for  $\gamma \rightarrow \infty$ . Figure 5 shows the temperature range close to  $T_c$ ; far below  $T_c$  the influence of fluctuations is negligible and all the curves should coalesce. For every temperature, we note that as  $\gamma$  increases from 0 to  $\infty$ ,  $\langle I(T) \rangle$  changes from  $\langle I_0(T) \rangle$  to  $\langle I_\infty(T) \rangle$ . However, this change is not monotonic:  $|\langle I(T) \rangle|$  initially decreases and after reaching a minimum increases toward  $|\langle I_\infty(T) \rangle|$ . The fact that  $|\langle I_0(T) \rangle| < |\langle I_\infty(T) \rangle|$  for  $T \approx T_c$  may look surprising, since  $\gamma = 0$  means larger freedom than  $\gamma \rightarrow \infty$  and we would therefore expect larger fluctuations in the former case. We will see in the following that indeed the order parameters assume larger values for  $\gamma = 0$ ; however, they may be less coordinated, resulting in a smaller current.

The solid curves in Fig. 6 show the values of  $\varphi$  for which the current is maximum at  $T = T_c$  for the limiting cases  $\gamma = 0$  and  $\gamma \rightarrow \infty$ . From a dimensional analysis we find that in the present situation the temperature enters the operator  $H/S$  only through the combination  $k_B T_c b R^3 / w$ , so that  $\varphi_{\text{max}}$  is a function of this quantity. Since the mean-field current has its maximum at  $\varphi_{\text{max}} > 1/4$ , it is interesting to note that  $\varphi_{\text{max}}$  can be smaller than  $1/4$ . The curve for  $\gamma \rightarrow \infty$  can be inferred from the case  $\gamma = 0$ : in order to obtain it at a given  $T_c$ , we have to double the value of  $w$ . Since  $\varphi_{\text{max}}$  is a function of  $k_B T_c b R^3 / w$ , doubling  $w$  is the same as dividing  $T_c$  by 2, i.e., at a given  $T_c$ , the value of  $\varphi_{\text{max}}$  for  $\gamma \rightarrow \infty$  is the same that  $\varphi_{\text{max}}$  for  $\gamma = 0$  had at half

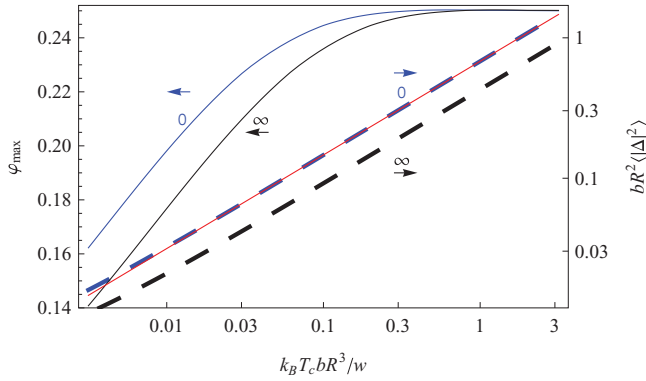


FIG. 6. (Color online) Magnetic flux for which the fluctuation current is maximal, and value of the order parameters at  $T = T_c$ , as functions of  $T_c$ .  $\langle |\Delta|^2 \rangle$  was evaluated at  $\varphi = \varphi_{\max}$ . Each curve is marked by its value of  $\gamma$  and by an arrow that points to the relevant  $y$  axis. The thin straight line (red online) highlights the asymptotic power dependence of  $bR^2 \langle |\Delta|^2 \rangle$  on  $k_B T_c b R^3 / w$ .

that temperature. With a logarithmic  $x$  axis, this relation gives a shift of the curve to the right.

The dashed lines in Fig. 6 show the values of  $bR^2 \langle |\Delta|^2 \rangle$  at  $T = T_c$  and  $\varphi = \varphi_{\max}$ , evaluated by means of Eq. (14). Except for  $k_B T_c \ll w/bR^3$  or  $k_B T_c \gg w/bR^3$ , we obtain  $\langle |\Delta|^2 \rangle \approx 0.68(bR^2)^{-1}(k_B T_c b R^3 / w)^{2/3} = 0.68(k_B^2 T_c^2 / bw^2)^{1/3}$  for  $\gamma = 0$ . For  $\gamma \rightarrow \infty$   $\langle |\Delta|^2 \rangle$  is smaller by a factor  $2^{2/3}$ . The first term in the Hartree approximation value in Eq. (27) is smaller than the result obtained for  $\gamma \rightarrow \infty$  by about 7%.

Figure 7 shows the average current evaluated at  $T = T_c$  and  $\varphi = \varphi_{\max}$ . As already found in Ref. 5,  $\langle I(T_c) \rangle$  is not a monotonic function of  $T_c$ , but has a maximum instead. As discussed above, the curve for  $\gamma \rightarrow \infty$  is obtained as a shift of the curve for  $\gamma = 0$ . What we learn from this curve is that for  $k_B T_c < 0.163w/bR^3$   $|\langle I_0(T_c) \rangle| > |\langle I_\infty(T_c) \rangle|$ , meaning that independence of the order parameters *enhances* the fluctuation current, whereas the *opposite* occurs for  $k_B T_c > 0.163w/bR^3$ .

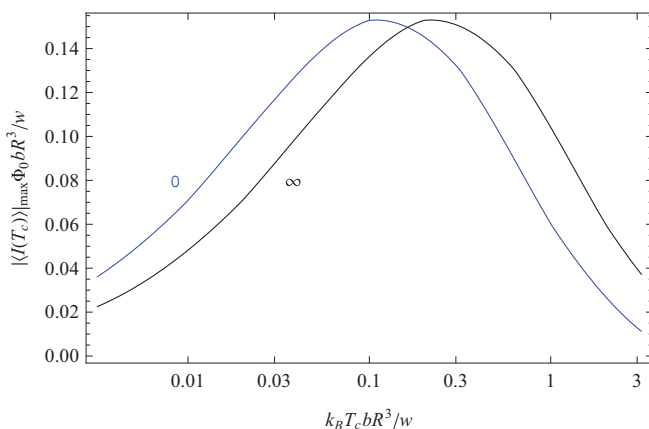


FIG. 7. (Color online) Maximum current at  $T = T_c$  as a function of the scaled  $T_c$  for  $\gamma = 0$  and for  $\gamma \rightarrow \infty$ .

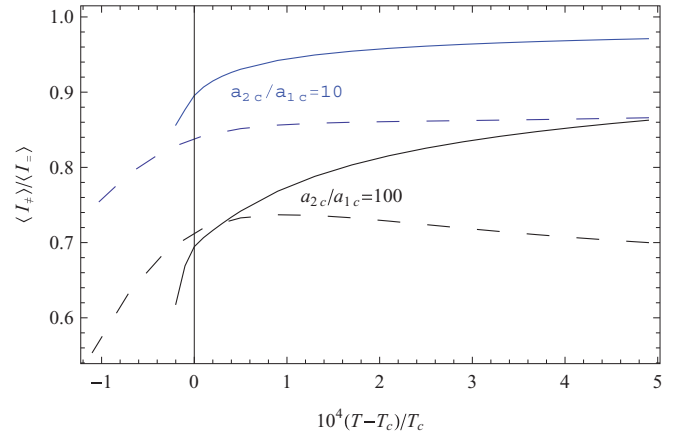


FIG. 8. (Color online) Ratio between the fluctuation currents for the case  $a_{1c} \neq a_{2c}$  (denoted  $I_{\neq}$ ) and the case  $a_{1c} = a_{2c}$  (denoted  $I_{=}$ ). For the solid lines  $b = 3 \times 10^{15} \text{ erg}^{-1} \text{ cm}^{-1}$  ( $k_B T_c b R^3 / w = 0.03$ ) and  $\gamma = 3 \times 10^6 \text{ cm}^{-2}$ ; for the dashed lines  $b = 10^{17} \text{ erg}^{-1} \text{ cm}^{-1}$  ( $k_B T_c b R^3 / w = 1$ ) and  $\gamma = 3 \times 10^7 \text{ cm}^{-2}$ . In all cases  $\varphi = \varphi_{\max}$ . The other parameters are the same as in Fig. 5.

## B. Asymmetric case

There are three material parameters that can differ between the order parameters:  $a_{1c} \neq a_{2c}$ ,  $\alpha_1 \neq \alpha_2$ , and  $b_1 \neq b_2$ . Since near  $T_c$  the usual case is  $|\alpha_{1,2}\tau|, b_{1,2}|\Delta_{1,2}|^2 \ll |a_{1c} - a_{2c}|$ , we focus on the influence of the difference between  $a_{1c}$  and  $a_{2c}$ .

Figure 8 shows the ratio between the fluctuation currents for the cases  $a_{1c} \neq a_{2c}$  and  $a_{1c} = a_{2c}$ , while all the other parameters are kept unchanged. Although the values of  $k_B T_c b R^3 / w$  and  $\gamma$  do have some influence, the general trend is that the difference between  $a_{1c}$  and  $a_{2c}$  inhibits fluctuation supercurrent in the region  $T \approx T_c$ , with this effect being stronger for  $T < T_c$ .

## C. Phase difference

The possibility of having two order parameters with different phases is a new degree of freedom not encountered in single band superconductors. This freedom could lead to novel phenomena and applications, and a broad spectrum of ideas have been raised in recent years (e.g., Refs. 28–31 and references therein).

In the language developed in Sec. II, the phase difference between the order parameters is  $\vartheta_1 - \vartheta_2$ ; our formalism enables easy investigation of the average value of  $\cos(\vartheta_1 - \vartheta_2)$ . Let us consider a material with  $\gamma > 0$ . Considerably below  $T_c$  the order parameters are large, the coupling interaction is large compared to the thermal energy, and the order parameters are practically locked, so that we expect  $\langle \cos(\vartheta_1 - \vartheta_2) \rangle \approx 1$ . In the opposite limit the coupling is small in comparison to the thermal energy, the order parameters are practically independent and  $\langle \cos(\vartheta_1 - \vartheta_2) \rangle \approx 0$ .

The values of  $\langle \cos(\vartheta_1 - \vartheta_2) \rangle$  were obtained by means of Eq. (14). Figure 9 shows these values as a function of temperature for material parameters as in  $\text{MgB}_2$ , in the absence of magnetic flux. The flux dependence would be hardly visible in the scale of this figure. The flux dependence vanishes both at low and at high temperatures and is largest close to

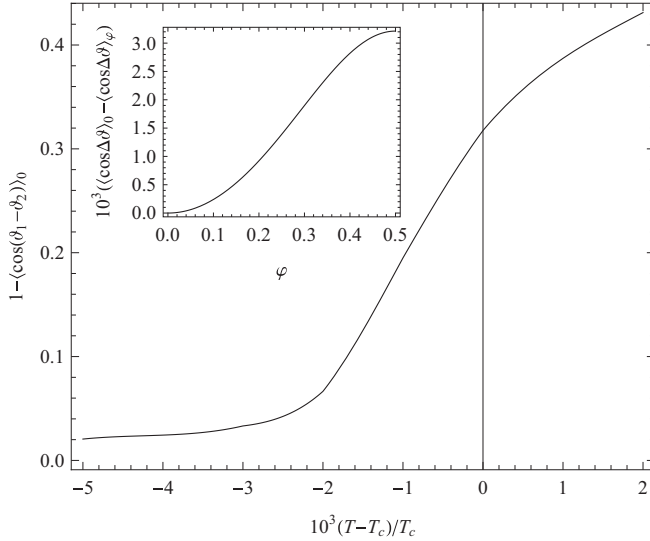


FIG. 9. Expectation values for the phase difference between both order parameters as a function of temperature for MgB<sub>2</sub> in the absence of flux. The material and geometric parameters are as in Fig. 1. Inset: dependence of the phase difference on the flux for  $T - T_c = -2 \times 10^{-3}T_c$ .  $\Delta\vartheta$  stands for  $\vartheta_1 - \vartheta_2$ .

$T = T_c - 2 \times 10^{-3}T_c$ . The inset shows the flux dependence at this temperature.

Figure 9 describes the phase difference as an average of a local quantity. Another question of interest stems from the global manifestation of phase, i.e., we could ask what is the probability that the two order parameters have different winding numbers. The possibility of fractional vortex states arising from different winding numbers has been discussed in the literature (e.g., Refs. 32 and 33) for simply connected samples and a similar phenomenon can be expected for a sample with a ring topology. Since vorticity is not a linear functional of the order parameters, it is not amenable for treatment using the formalism of Sec. II and methods similar to those used in Ref. 22 seem more appropriate.

## V. CONCLUSIONS

Motivated by a recent surge in interest in the physics of coupled condensates in two-band superconductors, we have analyzed the role and importance of fluctuations in superconducting rings with two order parameters. We have extended the analysis of the fluctuative regime made by von Oppen and Riedel<sup>5</sup> for the single order-parameter case, based on the Ginzburg-Landau energy functional. Further, we have made semianalytic evaluations of the influence of fluctuations on the persistent current and on the order parameters in the ring, as functions of temperature, coupling between the order parameters, and magnetic flux. For guidance of future experiments, we have identified the ranges of parameters where fluctuations inhibit or enhance the persistent current in the ring, and pointed out the influence of the cross section of the ring as well as the influence of the freedom of the order parameters to undergo separate fluctuations. Although the influence of fluctuations is most important close to  $T_c$ ,

we have also studied the behavior far from  $T_c$ , providing a complete picture.

In addition to two-band materials, our findings apply to artificially made systems of two superimposed rings, as readily made in experiments that involve annular Josephson junctions. The present study can also serve as a general guideline for theoretical efforts and interpretations of experimental data in systems described by multiple order parameters in the fluctuative regime. It is also well known that thermal fluctuations are more pronounced in low-dimensional systems, which enhances the relevance of our results especially bearing in mind that even elementary (Pb, In, Sn) but nanoscale superconductors are always effectively multiband.<sup>19</sup> It is of current interest to reveal the confinement and temperature regimes that favor or inhibit thermal fluctuations in such nanostructures, and control their influence on, e.g., vortex matter,<sup>34</sup> transport properties,<sup>35</sup> or applicability as, e.g., photon detectors.<sup>36</sup> Further studies of such effects in samples made of bulk-multiband superconductors are bound to be interesting, although nanostructuring of materials such as MgB<sub>2</sub> and pnictides is still a formidable experimental challenge.

## ACKNOWLEDGMENTS

This research was supported by the Israel Science Foundation, Grant No. 249/10, the Flemish Science Foundation (FWO-VI), and the ESF network INSTANS. We are grateful to Andrei Varlamov and Felix von Oppen for their answers to our enquiries.

## APPENDIX: PROOF OF EQ. (8)

We denote by  $\boldsymbol{\rho}$  the four-dimensional vector  $(\mathbf{r}_1, \mathbf{r}_2)$ . We divide the ring into  $N$  segments,  $N \gg 1$ , and rewrite Eq. (5) as

$$\frac{F}{k_B T} = \frac{2\pi}{NS} \sum_{i=0}^{N-1} g(\boldsymbol{\rho}_{i+1}, \boldsymbol{\rho}_i), \quad (\text{A1})$$

with  $S = k_B T R / 2w$ ,  $\boldsymbol{\rho}_i = \boldsymbol{\rho}(2i\pi/N)$  and  $g(\boldsymbol{\rho}_{i+1}, \boldsymbol{\rho}_i) = V(\boldsymbol{\rho}_{i+1}) + (N^2/8\pi^2)|\boldsymbol{\rho}_{i+1} - \boldsymbol{\rho}_i|^2$ .

Since  $\tilde{\Delta}_{1,2}$  are single valued,  $\boldsymbol{\rho}_0$  is a function of  $\boldsymbol{\rho}_N$ . Let us write this constraint as  $\boldsymbol{\rho}_0 = \tilde{\boldsymbol{\rho}}_N$ . Therefore substitution of Eq. (A1) into Eq. (7) gives

$$Z = \int d\boldsymbol{\rho}_0 \dots d\boldsymbol{\rho}_N \delta(\boldsymbol{\rho}_0 - \tilde{\boldsymbol{\rho}}_N) \exp\left[-\frac{2\pi g(\boldsymbol{\rho}_1, \boldsymbol{\rho}_0)}{NS}\right] \dots \times \exp\left[-\frac{2\pi g(\boldsymbol{\rho}_N, \boldsymbol{\rho}_{N-1})}{NS}\right]. \quad (\text{A2})$$

Using the identity  $\delta(\boldsymbol{\rho} - \boldsymbol{\rho}') = \sum_n \Psi_n^*(\boldsymbol{\rho}) \Psi_n(\boldsymbol{\rho}')$ , where  $\{\Psi_n\}$  is any complete set of normalized states,  $Z$  becomes

$$Z = \sum_n \int d\boldsymbol{\rho}_N \Psi_n^*(\tilde{\boldsymbol{\rho}}_N) \times \int d\boldsymbol{\rho}_{N-1} \exp\left[-\frac{2\pi g(\boldsymbol{\rho}_N, \boldsymbol{\rho}_{N-1})}{NS}\right] \dots \times \int d\boldsymbol{\rho}_0 \exp\left[-\frac{2\pi g(\boldsymbol{\rho}_1, \boldsymbol{\rho}_0)}{NS}\right] \Psi_n(\boldsymbol{\rho}_0). \quad (\text{A3})$$



Choosing the set  $\{\Psi_n\}$  such that it fulfils the eigenvalue equation

$$\int d\rho_i \exp\left[-\frac{2\pi g(\rho_{i+1}, \rho_i)}{NS}\right] \Psi_n(\rho_i) = \exp\left[-\frac{2\pi \varepsilon_n}{NS}\right] \Psi_n(\rho_{i+1}), \quad (\text{A4})$$

Z reduces to

$$Z = \sum_n \exp\left[-\frac{2\pi \varepsilon_n}{S}\right] \int d\rho_N \Psi_n^*(\tilde{\rho}_N) \Psi_n(\rho_N), \quad (\text{A5})$$

which is equivalent to Eq. (8).

We still have to find a set of eigenstates that fulfils Eq. (A4). Expanding  $\Psi_n(\rho_i)$  in powers of  $\rho_i - \rho_{i+1}$  around  $\Psi_n(\rho_{i+1})$ , which is equivalent to an expansion in powers of  $N^{-1/2}$ , the integral in Eq. (A4) can be performed and  $\Psi_n$  is found to obey the eigenvalue equation<sup>23</sup>  $H\Psi_n = \varepsilon_n\Psi_n$ .

<sup>1</sup>A. I. Larkin and A. A. Varlamov, *Theory of Fluctuations in Superconductors* (Oxford University Press, London, 2009).

<sup>2</sup>B. Rosenstein and D. Li, *Rev. Mod. Phys.* **82**, 109 (2010).

<sup>3</sup>W. A. Little and R. D. Parks, *Phys. Rev. Lett.* **9**, 9 (1962).

<sup>4</sup>N. C. Koshnick, H. Bluhm, M. E. Huber, and K. A. Moler, *Science* **318**, 1440 (2007).

<sup>5</sup>F. von Oppen and E. K. Riedel, *Phys. Rev. B* **46**, 3203 (1992).

<sup>6</sup>G. Schwiete and Y. Oreg, *Phys. Rev. Lett.* **103**, 037001 (2009).

<sup>7</sup>F. Bouquet, R. A. Fisher, N. E. Phillips, D. G. Hinks, and J. D. Jorgensen, *Phys. Rev. Lett.* **87**, 047001 (2001); P. Szabó, P. Samuely, J. Kacmarčík, T. Klein, J. Marcus, D. Fruchart, S. Miraglia, C. Marcenat, and A. G. M. Jansen, *ibid.* **87**, 137005 (2001); M. Iavarone, G. Karapetrov, A. E. Koshelev, W. K. Kwok, G. W. Crabtree, D. G. Hinks, W. N. Kang, E.-Mi Choi, H. J. Kim, H.-J. Kim, and S. I. Lee, *ibid.* **89**, 187002 (2002).

<sup>8</sup>Y. Singh, A. Niazi, M. D. Vannette, R. Prozorov, and D. C. Johnston, *Phys. Rev. B* **76**, 214510 (2007); Y. Singh, C. Martin, S. L. Bud'ko, A. Ellern, R. Prozorov, and D. C. Johnston, *ibid.* **82**, 144532 (2010).

<sup>9</sup>M. L. Teague, G. K. Drayna, G. P. Lockhart, P. Cheng, B. Shen, H.-H. Wen, and N.-C. Yeh, *Phys. Rev. Lett.* **106**, 087004 (2011); H. Kim, M. A. Tanatar, Y. J. Song, Y. S. Kwon, and R. Prozorov, *Phys. Rev. B* **83**, 100502(R) (2011).

<sup>10</sup>H. Bluhm, N. C. Koshnick, M. E. Huber, and K. A. Moler, *Phys. Rev. Lett.* **97**, 237002 (2006).

<sup>11</sup>See, e.g., A. Davidson, B. Dueholm, B. Kryger, and N. F. Pedersen, *Phys. Rev. Lett.* **55**, 2059 (1985); E. Kavoussanaki, R. Monaco, and R. J. Rivers, *ibid.* **85**, 3452 (2000); A. V. Ustinov, C. Coqui, A. Kemp, Y. Zolotaryuk, and M. Salerno, *ibid.* **93**, 087001 (2004).

<sup>12</sup>B. T. Geilikman, R. O. Zaitsev, and V. Z. Kresin, *Sov. Phys. Solid State* **9**, 642 (1967) [*Fiz. Tverd. Tela* **9**, 821 (1967)].

<sup>13</sup>M. E. Zhitomirsky and V.-H. Dao, *Phys. Rev. B* **69**, 054508 (2004).

<sup>14</sup>V. G. Kogan and J. Schmalian, *Phys. Rev. B* **83**, 054515 (2011).

<sup>15</sup>A. A. Shanenko, M. V. Milošević, F. M. Peeters, and A. V. Vagov, *Phys. Rev. Lett.* **106**, 047005 (2011).

<sup>16</sup>L. Komendová, M. V. Milošević, A. A. Shanenko, and F. M. Peeters, *Phys. Rev. B* **84**, 064522 (2011).

<sup>17</sup>W. Lawrence and S. Doniach, *Theory of Layer Structure Superconductors, Proceedings of the 12th International Conference on*

*Low Temperature Physics* (Academic Press of Japan, Kyoto, 1971), pp. 361–362.

<sup>18</sup>A. Gurevich, *Phys. Rev. B* **67**, 184515 (2003).

<sup>19</sup>Y. Guo, Y.-F. Zhang, X.-Y. Bao, T.-Z. Han, Z. Tang, L.-X. Zhang, W.-G. Zhu, E. G. Wang, Q. Niu, Z. Q. Qiu, J.-F. Jia, Z.-X. Zhao, and Q.-K. Xue, *Science* **306**, 1915 (2004); D. Eom, S. Qin, M. Y. Chou, and C. K. Shih, *Phys. Rev. Lett.* **96**, 027005 (2006).

<sup>20</sup>A. Gurevich, *Physica C* **456**, 160 (2007).

<sup>21</sup>V. Stanev and Z. Tešanović, *Phys. Rev. B* **81**, 134522 (2010).

<sup>22</sup>J. Berger, *J. Phys.: Condens. Matter* **23**, 225701 (2011).

<sup>23</sup>D. J. Scalapino, M. Sears, and R. A. Ferrell, *Phys. Rev. B* **6**, 3409 (1972).

<sup>24</sup>This is due to the fact that in the absence of fluctuations thermodynamic quantities are determined by the derivatives of  $F$  with respect to  $r_{1,2}^2$ , which in one case give  $b_{1,2}r_{1,2}^2$  and in the other, the equivalent  $b_{1,2}(r_{1,2}^2)$ .

<sup>25</sup>A. A. Golubov, J. Kortus, O. V. Dolgov, O. Jepsen, Y. Kong, O. K. Andersen, B. J. Gibson, K. Ahn, and R. K. Kremer, *J. Phys.: Condens. Matter* **14**, 1353 (2002).

<sup>26</sup>B. D. Tinh, D. Li, and B. Rosenstein, *Phys. Rev. B* **81**, 224521 (2010).

<sup>27</sup>V. Ambegaokar and U. Eckern, *Europhys. Lett.* **13**, 733 (1990).

<sup>28</sup>Y. Tanaka, *Phys. Rev. Lett.* **88**, 017002 (2001).

<sup>29</sup>A. Gurevich and V. M. Vinokur, *Phys. Rev. Lett.* **97**, 137003 (2006).

<sup>30</sup>A. Brinkman and J. M. Rowell, *Physica C* **456**, 188 (2007).

<sup>31</sup>A. Omelyanchouk in *Coherent Current States in Two-Band Superconductors*, Superconductivity-Theory and Applications, edited by Adir Moysés Luiz (InTech, Rijeka, Croatia, 2011).

<sup>32</sup>E. Babaev, *Phys. Rev. Lett.* **89**, 067001 (2002).

<sup>33</sup>R. Geurts, M. V. Milošević, and F. M. Peeters, *Phys. Rev. B* **81**, 214514 (2010).

<sup>34</sup>W. V. Pogosov, *Phys. Rev. B* **81**, 184517 (2010); W. V. Pogosov, V. R. Misko, and F. M. Peeters, *ibid.* **82**, 054523 (2010).

<sup>35</sup>I. Sochnikov, A. Shaulov, Y. Yeshurun, G. Logvenov, and I. Božović, *Nat. Nanotech.* **5**, 516 (2010).

<sup>36</sup>H. Bartolf, A. Engel, A. Schilling, K. Ilin, M. Siegel, H.-W. Hubers, and A. Semenov, *Phys. Rev. B* **81**, 024502 (2010).